STATISTICAL INVESTIGATION OF MAGNETO-HYDRODYNAMIC TURBULENCE DESCRIBED BY SPACE-TIME FUNCTIONAL FORMALISM- II

Kirti Sahu

Department of Mathematics, St. Vincent Pallotti College of Engineering and Technology, Nagpur-441108(India)

ABSTRACT

Joshi N. E. and Meshram M. C. derived the equations describing the dynamics of the kinetic energy spectrum density function and the magnetic energy spectrum density function on using the Lewis–Kraichnan space–time version of the Hopf functional formalism and the multiple-scale-cumulant expansion method for their investigation of Magnetohydrodynamic turbulence . Meshram M.C. and Sahu K. have written these equations in dimensionless form with respect to a representative wavenumber k_0 and a representative value of the energy spectrum E_0 and then integrated these equations numerically. The statistical quantities which were not included there (namely skewness, enstropy and Taylor's micro-scale of both the velocity field and the magnetic field for the representative value of Reynolds number R=20 and R=1600) are evaluated in the present work. We also discover the laws governing these statistical quantities. Further, we discuss the merits and scope of the present closure scheme for studying similar types of turbulent flows.

Keywords* : *Closure Method , Energy Specturm Function, MHD Turbulence, Statistical Quantities

I INTRODUCTION

Turbulence is a ubiquitous phenomenon. Turbulent fluid flows are experienced in daily life. When the fluid is electrically conducting, the turbulent motions are accompanied by magnetic field fluctuations and give rise to magnetohydrodynamic turbulence. G.K. Batchelor[1] and S. Chandrasekhar[2,3,4] have shown that the phenomenological theory of turbulence in magnetohydrodynamics can be developed to same extent as the corresponding theories in ordinary hydrodynamic turbulence developed by Taylor[5], Von Karman and Howarth[6], Robertson[7], Kolmogoroff[8], Batchelor[1] and Heisenberg[9]. Hence, concepts and techniques that have evolved in fully developed hydrodynamical turbulence can be extended to other strongly non-linear problems. Functional calculus for the theory of hydrodynamic turbulence was first introduced by E Hopf[10]. K. Goto[11] extended this theory to the magnetohydrodynamic turbulence. R.M. Lewis and R.H. Kraichnan[12] gave the space-time functional formalism of Hopf equation. N.E.Joshi and S.V. Krishna[13] translated this functional formalism for magnetohydrodynamic turbulence and obtained two equations for characteristic functional of the joint probability distribution of the velocity and magnetic fields. G.Ahmadi[14] offered approximate methods for Burger's model of hydrodynamic turbulence based on series expansion of the natural logarithm of characteristic functional. N.E. Joshi and M.C. Meshram[15] extended Ahmadi's version to

magnetohydrodynamic turbulence and obtained a closed set of cumulant equations in real space using zero-fourth-order-cumulant approximation. N.N. Bogoliubov[16] originated a method of multiple time scale expansion. W.M.P Malfliet[17] was first to apply this method of multiple time scales to Burgers hydrodynamic turbulence. T. Tatsumi, S. Kida and J. Mizushima[18] applied multiple-scale-cumulant-expansion method to an incompressible isotropic turbulence and obtained positive definite energy spectrum at all Reynolds numbers. N.E. Joshi and M.C. Meshram[15] have raised the domain to space-time functional which indeed is essential in order to extend this concept to hydromagnetic turbulence.

In section 2 a close set of equations for the energy spectrum functions for MHD turbulence in dimensionless form are considered from M.C.Meshram and K.Sahu[19]. The equations for energy spectrum functions are integrated numerically and the statistical quantities describing the MHD turbulence such as the energy transfer function, energy dissipation function, enstrophy , Taylor's micro-scale and the skewness are evaluated from the numerical values of energy spectrum function of velocity field and magnetic field and a detail analysis of these quantities is presented in section 3. In section 4 we write the summary and discuss the merit of results obtained which is followed by the scope of the method for conducting further research.

II EQUATIONS FOR THE ENERGY SPECTRUM FUNCTIONS IN DIMENSIONLESS FORM

M.C. Meshram and K.Sahu[19] obtained the following equations describing the dynamics of the kinetic energy spectrum density function and the magnetic energy spectrum density function in dimensionless form with respect to a representative wavenumber k_0 and a representative value of the energy spectrum E_0 :

$$\left(\frac{\partial}{\partial \tau}+\frac{\kappa^2}{R}\right)\phi^V(\kappa,\tau)=4\pi R\int_{-\infty}^{\infty}d\kappa'\int_{-1}^{1}\frac{1-e^{-\left(\kappa^2+\kappa'^2+\kappa''^2\right)\tau/R}}{\left(\kappa^2+\kappa'^2+\kappa''^2\right)}\kappa\kappa'^3\left(\frac{\kappa\kappa'}{\kappa''^2}+\mu\right)\left(1-\mu^2\right)$$
$$\{\left(\phi^V(\kappa',\tau)-\phi^V(\kappa,\tau)\right)\phi^V(\kappa'',\tau)-\left(\phi^M(\kappa',\tau)-\phi^M(\kappa,\tau)\right)\phi^M(\kappa'',\tau)\}\,d\mu \quad (2.1a)$$

$$\left(\frac{\partial}{\partial \tau}+\frac{\kappa^2}{R}\right)\phi^M(\kappa,\tau)=4\pi R\int_{-\infty}^{\infty}d\kappa'\int_{-1}^{1}\frac{1-e^{-\left(\kappa^2+\kappa'^2\right)\tau/R}}{\left(\kappa^2+\kappa'^2\right)}$$
$$\{\kappa(\kappa+\kappa'\mu^3)\phi^V(\kappa',t)\phi^M(\kappa,\tau)-\kappa'(\kappa'+\kappa\mu^3)\phi^V(\kappa,\tau)\phi^M(\kappa',\tau)$$
$$-\kappa^2\left(1+\frac{\kappa'}{\kappa''^2}(\kappa+\kappa'\mu)(1-\mu^2)\right)\left(\phi^V(\kappa',\tau)-\phi^V(\kappa,\tau)\right)\phi^M(\kappa'',\tau)\}\,d\mu$$

(2.1b)

Where $\kappa''^2=\kappa^2+\kappa'^2+2\mu\kappa\kappa'$

They solved these equations numerically by using the following initial conditions for energy density functions

$$\phi^{V}(\kappa,0)=\frac{1}{4*pi}\exp(-\kappa^{2}) \quad \text{and} \quad \phi^{M}(\kappa,0)=\frac{1}{400*pi}\exp(-\kappa^{2}) \tag{2.2}$$

Also, they selected the following initial conditions for energy spectrum functions $E^{V}(k,t)$ *and* $E^{M}(k,t)$:

$$E^{V}(k,0)=E_{0}^{V}\left(k/k_{0}\right)^{2}\exp\left[-\left(k/k_{0}\right)^{2}\right] \quad \text{and} \quad E^{M}(k,0)=E_{0}^{M}\left(k/k_{0}\right)^{2}\exp\left[-\left(k/k_{0}\right)^{2}\right] \tag{2.3}$$

The integrals on the right –hand side of (2.1a) and (2.1b) are calculated numerically by using appropriate sum rules at discrete values of κ' and μ and terminating the infinite integrals with respect to κ' at a sufficiently large value of κ'. At very large Reynolds number the integrand changes rapidly at small κ' and does not vanish even at large κ'. In order to evaluate such an integral accurately and efficiently we employ a non–uniform mesh for κ' whose size is an increasing function of κ'.

The following variables are introduced for this purpose:

$$\xi=\log(10\kappa) \qquad \eta=0.01R\tau \qquad \phi(\xi,\eta)=0.1\phi(\kappa,\tau) \tag{2.4}$$

In terms of these new variables equations (2.1a) and (2.1b)

$$\left(\frac{\partial}{\partial\eta}+\frac{e^{2\xi}}{R^{2}}\right)\phi^{V}(\xi,\eta)$$

$$=3\pi\int_{-\infty}^{\infty}e^{3\xi'}d\xi'\int_{-1}^{1}\left(\frac{1-\exp\left[-2e^{\xi+\xi'}\left(e^{\xi-\xi'}+e^{\xi'-\xi}+\mu\right)\eta/R^{2}\right]}{e^{\xi-\xi'}+e^{\xi'-\xi}+\mu}\right)\left(\frac{1}{e^{\xi-\xi'}+e^{\xi'-\xi}+2\mu}+\mu\right)\left(1-\mu^{2}\right)$$

$$\times\left\{\left(\phi^{V}(\xi',\eta)-\phi^{V}(\xi,\eta)\right)\phi^{V}(\xi'',\eta)-\left(\phi^{M}(\xi',\eta)-\phi^{M}(\xi,\eta)\right)\phi^{M}(\xi'',\eta)\right\}d\mu \tag{2.5a}$$

$$\left(\frac{\partial}{\partial\tau}+\frac{e^{2\xi}}{R^{2}}\right)\phi^{M}(\xi,\eta)=3\pi\int_{-\infty}^{\infty}d\xi'\int_{-1}^{1}\left(\frac{1-\exp\left[-e^{\xi+\xi'}\left(e^{\xi-\xi'}+e^{\xi'-\xi}\right)\eta/R^{2}\right]}{e^{\xi-\xi'}+e^{\xi'-\xi}}\right)\times$$

$$\left\{\left(e^{\xi}+e^{\xi'}\mu^{3}\right)\phi^{V}(\xi',\eta)\phi^{M}(\xi,\eta)-\left(e^{\xi'}+e^{\xi}\mu^{3}\right)\phi^{M}(\xi',\eta)\phi^{V}(\xi,\eta)\right.$$

$$\left.-e^{\xi}\left(1+\frac{(1+e^{\xi'-\xi}\mu)(1-\mu^{2})}{e^{\xi-\xi'}+e^{\xi'-\xi}+2\mu}\right)\left(\phi^{V}(\xi',\eta)-\phi^{V}(\xi,\eta)\right)\phi^{M}(\xi'',\eta)\right\}d\mu$$

(2.5b)

III EVALUATION OF STATISTICAL QUANTITIES AND GOVERNING LAWS

The infinite integral with respect to ξ' is terminated at $\xi' = \Sigma + \log 2 \quad (\kappa' = 0.2)$ and calculated by Simpsons rule in the region $-\Sigma < \xi' \leq \Sigma$ with a mesh size $\Delta\xi' = 0.01$. The following values have been chosen for Σ :

$$\Sigma = \begin{cases} 30 & R = 5,10,20,100 \\ 40 & for \quad R = 200,400 \\ 45 & R = 800,1600 \end{cases}$$

These values of Σ have been confirmed to be sufficiently large by numerical results .The integration with respect to μ is carried out by Simpson rule with a mesh size $\Delta\mu = 0.1$ .The derivative $\frac{\partial}{\partial \eta}$ is replaced by the forward–difference quotient with mesh size $\Delta\eta = 0.0002R$ .Thus, the equations (2.5a) and (2.5b) are solved numerically for the initial conditions(2.2) ; the Reynolds number R=20 and R=1600; and the energy spectrum functions $E^V(k,t)$ *and* $E^M(k,t)$ are obtained as functions of the wavenumber k and time t. Important statistical quantities characterizing magneto-hydrodynamic turbulence are derived from numerical results for energy spectrum functions for velocity field and magnetic field are as defined below:

Energy spectrum function: $E^V(k,t) = 4\pi k^2 \phi^V(k,t)$ and $E^M(k,t) = 4\pi k^2 \phi^M(k,t)$

Ratio of magnetic to kinetic energy spectrum function: $\psi(k,t) = \frac{E^M(k,t)}{E^V(k,t)}$

Energy transfer functions:

$$T^V(k,t) = 4\pi k^2 \left(\frac{\partial}{\partial t} + 2\gamma k^2 \right) \phi^V(k,t) \text{ and } T^M(k,t) = 4\pi k^2 \left(\frac{\partial}{\partial t} + 2\gamma k^2 \right) \phi^M(k,t)$$

Enstropy : $\varepsilon^V(t) = 4\pi \int_0^\infty k^2 \phi^V(k,t)\,dk$ and $\varepsilon^M(t) = 4\pi \int_0^\infty k^2 \phi^M(k,t)\,dk$

Energy dissipation function: $D^V(k,t) = 2\nu k^2 E^V(k,t)$ and $D^M(k,t) = 2\nu k^2 E^M(k,t)$

Skewness: $S^V(t) = \frac{3\sqrt{30}}{14} \frac{5\int_0^\infty k^2 T^V(k,t)\,dk}{\left[\int_0^\infty k^2 E^V(k,t)\,dk\right]^{3/2}}$ and $S^M(t) = \frac{3\sqrt{30}}{14} \frac{5\int_0^\infty k^2 T^M(k,t)\,dk}{\left[\int_0^\infty k^2 E^M(k,t)\,dk\right]^{3/2}}$

Taylor's Microscale: $\lambda^V(t) = \frac{5\int_0^\infty E^V(k,t)\,dk}{\int_0^\infty k^2 E^V(k,t)\,dk}$ and $\lambda^M(t) = \frac{5\int_0^\infty E^M(k,t)\,dk}{\int_0^\infty k^2 E^M(k,t)\,dk}$

The numerical integration of (2.5a)–(2.5b) uncovers following laws for the magnetohydrodynamic turbulence.

In the lowest subrange of the universal wavenumber range, the kinetic energy spectrum function and magnetic energy spectrum function both are proportional to -5/3 power of the wave number in the inertial range.

These laws are symbolically written as follows:

$$E^{V}(k,t) \propto k^{-\frac{5}{3}} \; ; \; E^{M}(k,t) \propto k^{-\frac{5}{3}} \tag{3.1}$$

These energy spectrum function has exactly the same power as Kolomogorov's inertial- subrange spectrum. Next to previous subrange, there exists a subrange in which the energy spectrum functions of both the velocity field and magnetic field are inversely proportional to a wavenumber. These laws are symbolically written as follows:

$$E^{V}(k,t) \propto k^{-1} \; ; \; E^{M}(k,t) \propto k^{-1} \tag{3.2}$$

At still higher wave number, both the spectrum functions take the exponential form. Thus, the results obtained by the application of multiple–scale–cumulant–expansion method support the asymptotic decay of the spectrum functions for very high wavenumber irrespective of Reynolds numbers considered. The function $\psi(k,t)$ which is the ratio of magnetic energy to kinetic energy is shown in fig 3. From figure 3 it is clear that $\psi(k,t)$ grows monotonically to a value of 4 by t=1.2.The variation of $\psi(k,t)$ with time is linked to the magnetic Reynolds number of the flow. The enstropy of velocity field , $\varepsilon^{V}(t)$ and magnetic field , $\varepsilon^{M}(t)$ are plotted in figure 4 and figure 5 respectively. We infer from these graphs of enstropy that they are analogous to each other. The shape of each of these graphs can be divided into three parts depending upon their behaviour with respect to time. For R=20, the first part being from t = 0 to t =7, the second part from t =7 to t=15 and third part t=15 onwards. The enstropy for both the fields, $\varepsilon^{V}(t)$ and $\varepsilon^{M}(t)$ increase monotonically with respect to time in the initial period.

Thereafter, in the second period the curves attain the Gaussian shape. In the final period corresponding to t >15 the enstropy of both the velocity and magnetic field increases monotonically. We also observe from these figures that as the Reynolds number increases there is decrease in the time taken to attain the maximum enstropy in case of both the fields.

In the initial period before attaining the maximum value the enstropy of the velocity field is proportional to 2.2 power of time and analogues to this enstropy of the magnetic field are proportional to 2.27 power of time.

These laws symbolically are written as follows:

$$\varepsilon^{V}(t) \; \alpha \; t^{2.2} \; ; \; \varepsilon^{M}(t) \; \alpha \; t^{2.27} \tag{3.3}$$

Next to previous period just after attaining the maximum value for R=20 and R=1600 the value of enstropy of both the fields decreases and this decrease is governed by the following laws:

The enstropy of the velocity field is proportional to the negative 2.2 power of time and the enstropy of the magnetic field is proportional to the negative 2.25 power of time. These laws symbolically are written as follows

$$\varepsilon^{V}(t) \; \alpha \; t^{-2.2} \; ; \; \varepsilon^{M}(t) \; \alpha \; t^{-2.25} \tag{3.4}$$

These laws agree quite well with the experimental results. In the last period enstropy of the velocity field and magnetic field varies with respect to time as per the following laws:

The enstropy of the velocity field is proportional to the 1.03 power of time whereas the enstropy of the magnetic field is proportional to the 1.13 power of time. These laws symbolically are written as follows:

$$\varepsilon^{V}(t) \ \alpha \ t^{1.03} \ ; \ \varepsilon^{M}(t) \ \alpha \ t^{1.13} \tag{3.5}$$

The enstropy of magnetic field clearly grows more than enstropy of velocity field. From figure 6 and figure 7 showing the skewness of velocity field and magnetic field we infer that they are analogous to each other. The shape of each of these graphs can be divided into three parts depending upon their behaviour with respect to time. For R=20, the first part being from t = 0 to t =7, the second part from t =7 to t=15 and third part t=15 onwards. The skewness for both the fields, $S^{V}(t)$ and $S^{M}(t)$ increases monotonically with respect to time in the initial period .Thereafter in the second period the curves attain the Gaussian shape. In the final period corresponding to t >15 the skewness of both the velocity and magnetic field increases monotonically. We also observe from these figures that as the Reynolds number increases there is decrease in the time taken to attain the maximum skewness in case of both the fields.

For both the velocity and magnetic field their skewness grows very rapidly in the initial period and attains a quite large maximum value 0.37 for R=20 and 2.8 corresponding to R=1600 by velocity field. Similarly the corresponding maximum values for the magnetic field are 0.21 and 2.4 respectively. This reveals that there is a increase in the maximum value of skewness with rise in the Reynolds number.

In the initial period before attaining the maximum value the skewness of the velocity field is proportional to 2.2 power of time and an analogue to this skewness of the magnetic field is proportional to 2.27 power of time.

These laws symbolically are written as follows:

$$S^{V}(t) \ \alpha \ t^{2.2} \ ; S^{V}(t) \ \alpha \ t^{2.27} \tag{3.6}$$

Next to previous period just after attaining the maximum value for R=20 and R=1600 the value of skewness of both the field decreases and this decrease is governed by the following laws:

The skewness of the velocity field is proportional to the negative 2.2 power of time and the skewness of the magnetic field is proportional to the negative 2.25 power of time. These laws are symbolically written as follows:

$$S^{V}(t) \ \alpha \ t^{-2.2} \ ; \ S^{V}(t) \ \alpha \ t^{-2.25} \tag{3.7}$$

These laws agree quite well with the experimental results. In the last period skewness of the velocity field and magnetic field varies with respect to time as per the following laws:

The skewness of the velocity field is proportional to the 1.03 power of time whereas the skewness of the magnetic field is proportional to the 1.13 power of time. These laws are symbolically written as follows:

$$S^{V}(t) \ \alpha \ t^{1.03} \ ; \ S^{V}(t) \ \alpha \ t^{1.13} \tag{3.8}$$

From figure 6 and 7 we also notice that these skewness are a measure of the departure from Gaussianity , and indicate how transfer functions vary with the time at high wavenumber. They decrease substantially after having reached their sharp maximum and before stabilizing.

The energy dissipation function for kinetic energy and magnetic energy clearly exhibit the characteristic of energy spectra as shown in figure 8 and figure 9.

The transfer spectra of magnetic energy and kinetic energy depict in figure 10 and figure 11 behave differently. Both transfer spectra are positive in the first shell, indicating that an inverse transfer of magnetic energy is occurring at low wavenumber.

It is observed that for large Reynolds number, the energy containing range and the inertial subrange the energy dissipation is much smaller in magnitude than the energy transfer. For a given Reynolds number, in the neighbourhood of the wavenumber both the energy transfer functions change their sign satisfying the condition:

$$\int_0^\infty T^V(k,t)\,dk = 0 \quad ; \quad \int_0^\infty T^M(k,t)\,dk = 0 \tag{3.9}$$

as per the present closure scheme employed. Finally it is observed that the exponential spectrum occurs in the wavenumber range in which energy transfer is nearly balanced by the energy dissipation. A.Pouquet and G.S.Patterson[20] have investigated MHD turbulence numerically by restricting to magnetic Prandtl number of one and obtained results for Reynolds number 40 based on Taylor micro scale. The predictions of present closure scheme for magnetic Prandtl number one and Reynolds number as large as 1600 are in good agreement with those of the former.

The Taylor's microscale of the velocity field, $\lambda^V(t)$ and for the magnetic field, $\lambda^M(t)$ are plotted in figure 12 and figure 13. At large Reynolds numbers the micro-scale for the velocity field and that of the magnetic field decreases rapidly from its initial value to a minimum and then increases almost proportionally with time. The minimum value of the Taylor's micro-scale of the velocity field and that of the magnetic field is t=0.5 and t=0.6 for R=20 respectively and these values for R=1600 respectively are t=0.55 and t=0.65.

The decrease of the Taylor's micro-scale of the velocity field and that of the magnetic field with time is governed by the laws that the microscale of both the velocity field and magnetic field vary proportional to negative 0.5 power of the time. Symbolically these laws are

$$\lambda^V(t) \alpha \; t^{-0.5} \; ; \; \lambda^M(t) \alpha \; t^{-0.5} \tag{3.10}$$

The variation of the Taylor's micro-scale of the velocity field and that of the magnetic field with time confirms the asymptotic decrease of Taylor's micro-scale with time. Similarly the increase of the Taylor's micro-scale of the velocity field and that of the magnetic field with time is governed by the laws that the microscale of both the velocity field and magnetic field vary proportional to 0.5 power of the time. Symbolically these laws are

$$\lambda^{V}(t) \alpha \ t^{0.5} \ ; \lambda^{M}(t) \alpha \ t^{0.5} \qquad (3.11)$$

$\varepsilon^{M}(t)$

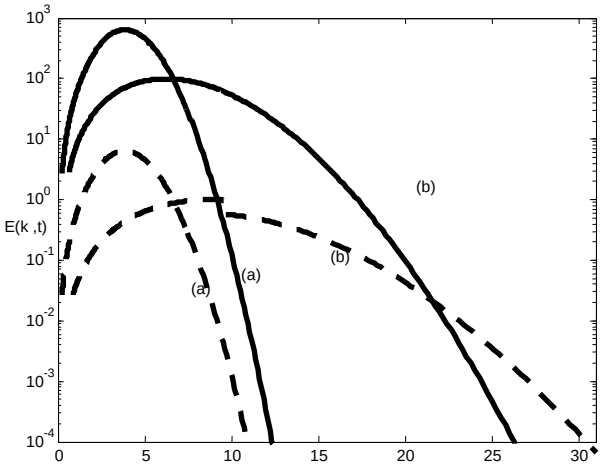

Figure 1. Kinetic (solid lines) and Magnetic (Dashed lines) energy spectrum function for R=20 at (a) t =0 and (b) t =3

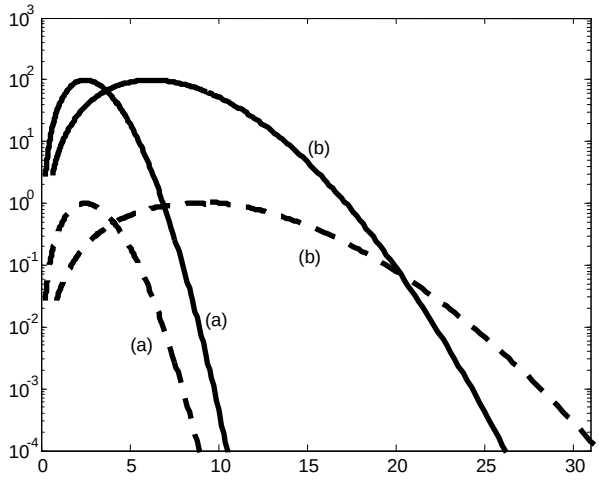

Figure 2. Kinetic (solid lines) and Magnetic (Dashed lines) energy spectrum function for R=1600 at (a) t =0 and (b) t =3

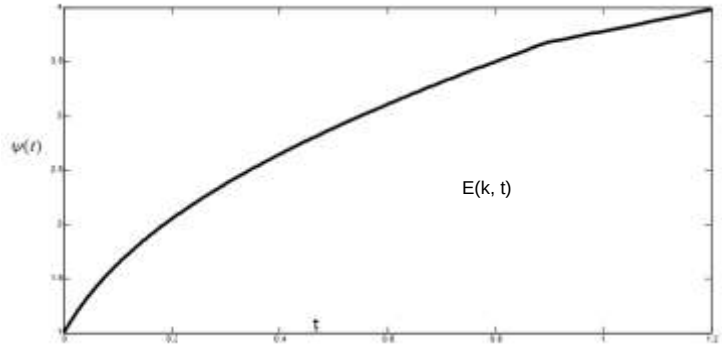

Figure 3. $\psi(t)$ ***verses time***

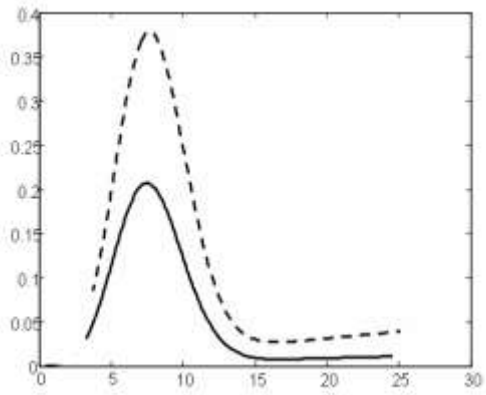

Figure 4. Enstropy for Velocity field (solid lines) *and Magnetic field (Dashed lines) at R=20*

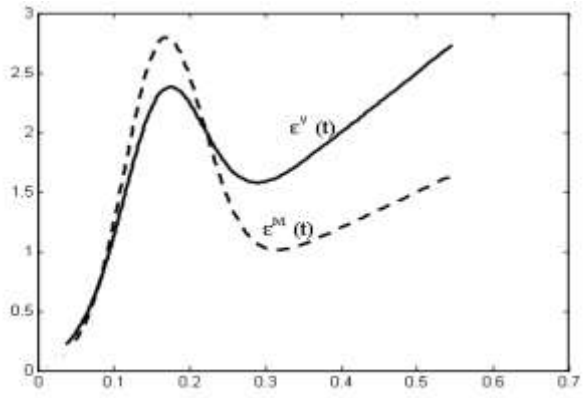

Figure 5. Enstropy for Velocity field (solid lines) *and Magnetic field (Dashed lines)at R=1600*

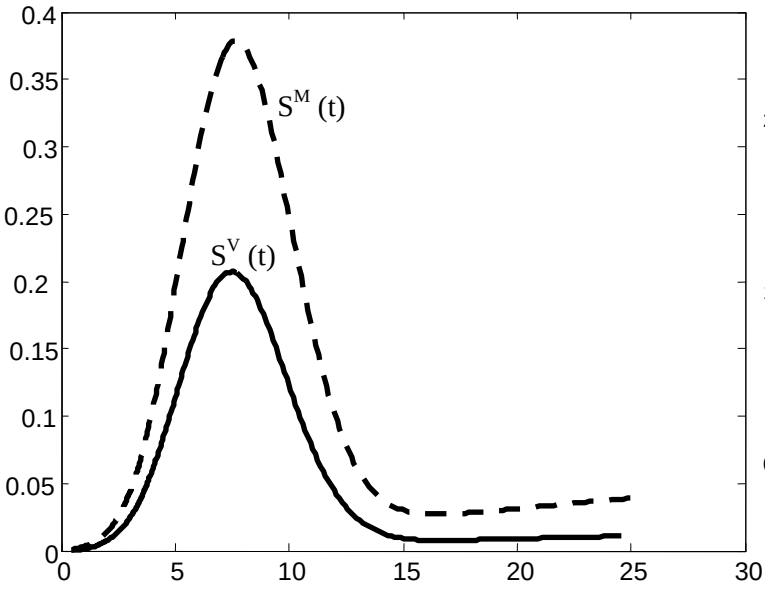

Figure 6. Skewness for for Velocity field (solid lines) Magnetic field (Dashed lines) at R=20

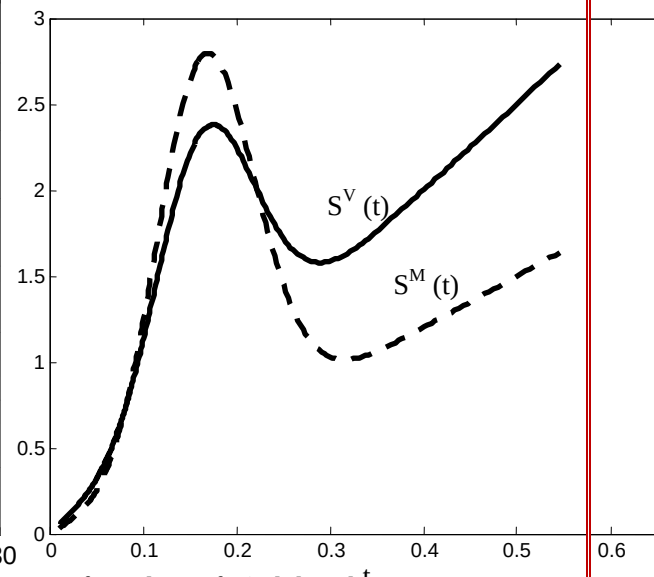

Figure 7. Skewness for Velocity fie(solid and Magnetic field (Dashed lines) at R=1600

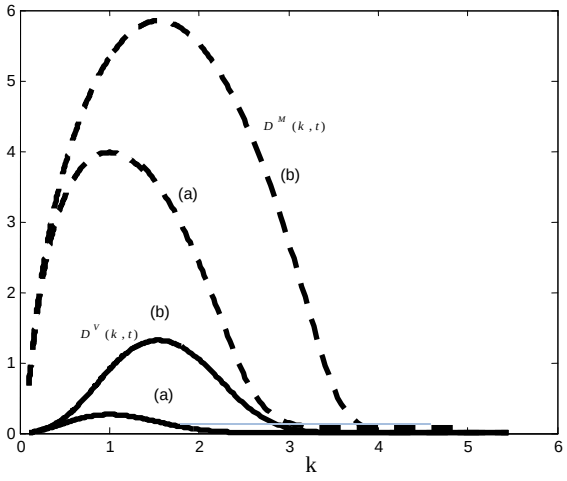

Figure 8. Energy dissipation function for R=20 at (a) t=0 and (b) t=3 ,

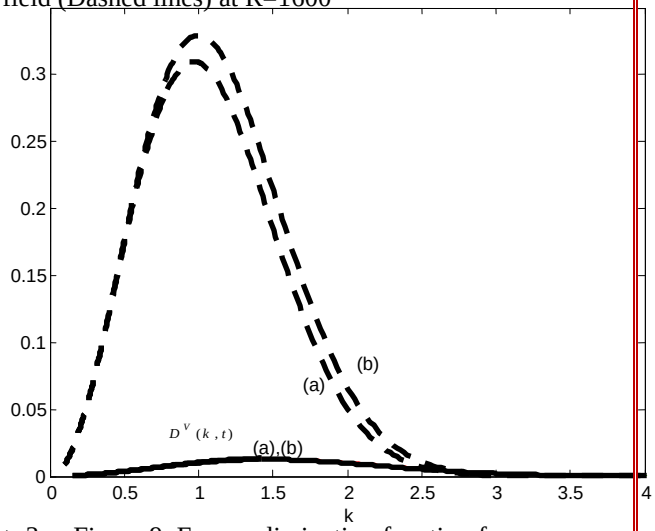

Figure 9. Energy dissipation function for R=1600 at (a) t=0 and (b) t=3

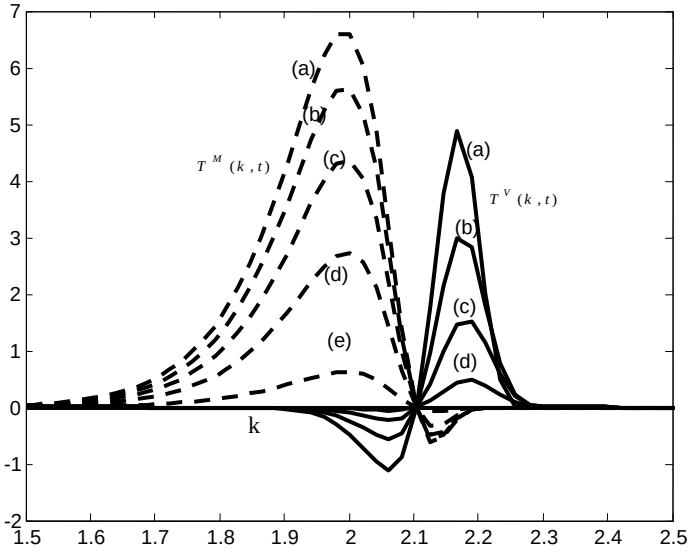

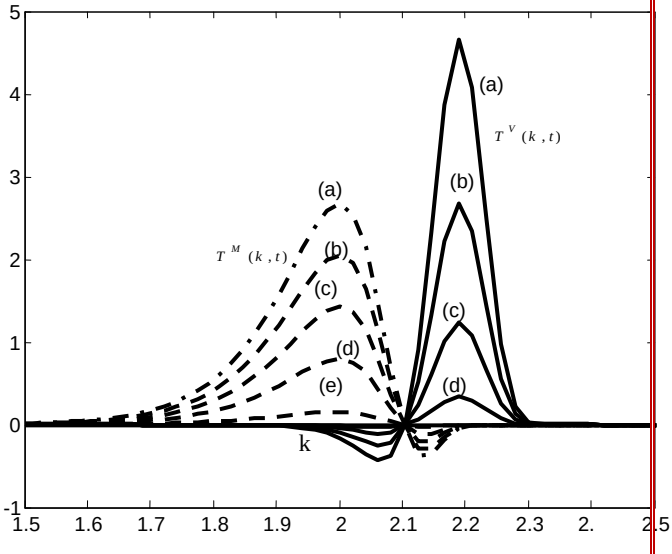

Figure 10. Kinetic (Solid lines) and Magnetic (dashed lines) energy transfer function for R=20 at (a) t =0 , (b) t=1 , (c) t=2 , (d) t=3 and (e) t=4

Figure 11. Kinetic (Solid lines) and Magnetic (dashed lines) energy transfer function for R=1600 at (a) t =0 , (b) t=1 (c) t=2 , (d) t=3 and (e) t=4

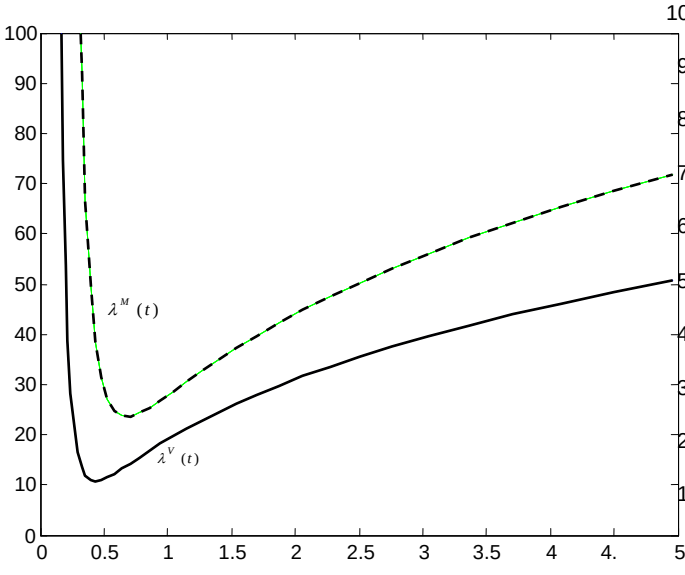

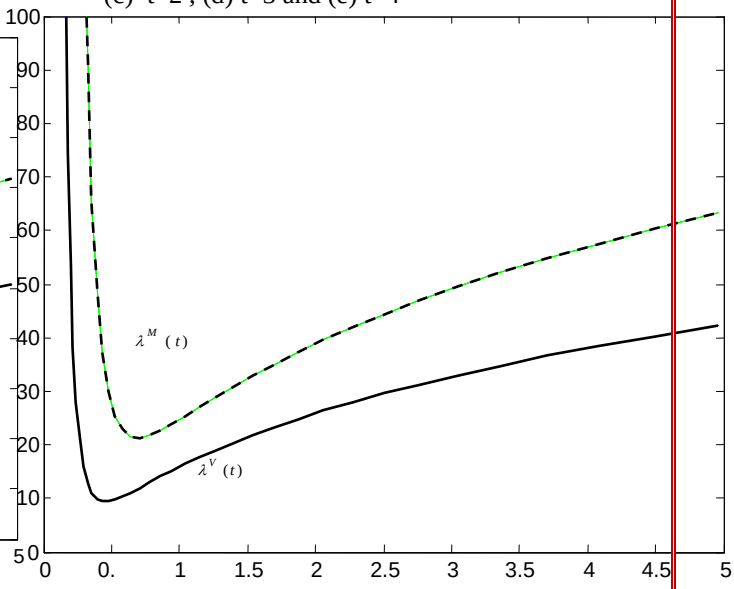

Figure 12. Kinetic (Solid lines) and Magnetic (dashed lines) energy transfer function for R=20 at (a) t =0 , (b) t=1 , (c) t=2 , (d) t=3 and (e) t=4

Figure 13. Kinetic (Solid lines) and Magnetic (dashed lines) energy transfer function for R=1600 at (a) t =0 , (b) t=1 (c) t=2 , (d) t=3 and (e) t=4

IV RESULTS

1. Both the kinetic energy spectrum function and the magnetic energy spectrum function are found to be positive definite for all values of Reynolds numbers R=20 and R=1600.

2. At large Reynolds numbers both the kinetic energy spectrum function and magnetic energy spectrum function take the form of Kolmogorov's -5/3 power spectrum in the inertial subrange , whose extent increases indefinitely with Reynolds number .In the higher wavenumber region beyond the inertial subrange the spectrum takes a universal form which is independent of its structure at lower wavenumbers.

3. The universal spectrums are composed of three different subspectra, which are in order of increasing wavenumber, the $k^{-5/3}$ spectrum, the k^{-1} spectrum and the exponential spectrum.

4. The ratio of magnetic energy to kinetic energy $\psi(t)$ which initially was 10^{-2}, is found as a monotonically growing function with respect to time. The variation of $\psi(t)$ with time is related to Reynolds number.

5. As Reynolds number increases the time required to attain the maximum value of enstropy also increases. For both the velocity and magnetic field their enstrophy grows very rapidly in the initial period and the velocity field attains a quite large maximum value. This reveals that there is an increase in the maximum value of enstropy with rise in the Reynolds number. In the initial period the enstropy of the velocity field is proportional to 2.2 power of time and analogues to this enstropy of the magnetic field is proportional to 2.27 power of time.In the intermediate period the enstropy of both the velocity and magnetic fields assumes the Gaussian shape and the enstropy of the velocity field is proportional to the negative 2.2 power of time and the enstropy of the magnetic field is proportional to the negative 2.25 power of time whereas in the third period the enstropy increases with

time and enstropy of the velocity field is proportional to the 1.03 power of time and the enstropy of the magnetic field is proportional to the 1.13 power of time. The enstropy of magnetic field grows more than the enstropy of velocity field.

6. The initial value of skeness is identically zero for both the reactants. In the initial period the the skewness of the velocity field is proportional to 2.2 power of time and analogues to this skewness of the magnetic field is proportional to 2.27 power of time. In the intermediate period the skewness of both the velocity and magnetic fields assumes the Gaussian shape and the skewness of the velocity field is proportional to the negative 2.2 power of time and the skewness of the magnetic field is proportional to the negative 2.25 power of time whereas in the third period the skewness increases with time .The skewness of the velocity field is proportional to the 1.03 power of time and the skewness of the magnetic field is proportional to the 1.13 power of time.

7. As Reynolds number increases the energy dissipation decreases in magnitude than the energy transfer. The transfer spectra of magnetic energy and kinetic energy behave differently. As the Reynolds number takes the larger value the wavenumber at which energy transfer function of both the field vanish is shifted to the lower wavenumber.

8. The Taylor's microscale of both the velocity field and magnetic field varies proportionally to 0.5 power of the time.

REFERENCES

[1] Batchelor G K 1950 *Proc. Roy. Soc.* A 201 405

[2] Chandrasekhar S 1951 *Proc. Roy. Soc.* A 204 435

[3] Chandrasekhar S 1951 *Proc. Roy. Soc.* A 207 301

[4] Chandrasekhar S 1955 *Proc. Roy. Soc.* A 233 322

[5] Taylor G I 1935 *Proc. Roy. Soc.* A 151 1

[6] Von Karman T and Howarth L 1938 *Proc. Roy. Soc.* A 164 192

[7] Robertson H P 1940 *Proc. Camb. Phil. Soc.* 36 209

[8] Kolmogoroff A N 1941 *Dokl. Akad. Nauk. SSSR* 32 16

[9] Heisenberg W 1948 *Proc. Roy. Soc.* A 195 402

[10] Hopf E 1962 *Symp. Appl. Math.* 13 157

[11] K. Goto. 1961 Prog. of Theoretical Phys. 25(4) 603

[12] Lewis R M and Kraichan R H 1962 *Commun. Pure Appl. Math.* 15 397

[13] Krishna S. V. and Joshi N. E. 1967 J. Math and Phys.Sci. 1(3) 207

[14] G.Ahmadi 1976 Appl. Sci. Res. 32 207

[15] Joshi N E and Meshram M C 1985 *30th Congress of ISTAM (New Delhi)* 167

[16] N. N. Bogoliubov 1962 Studies in Statistical Mechanics North Holand

[17] W.P.M. Malfliet 1969 Physics. 45 257

[18] T.Tatsumi, S.Kida and J.Mizushima 1977 J. fliud Mech. 31 97

[19] Meshram M.C. and Sahu K. 2013 Phys. Scr. T155 014044 1

[20] Pouquet A and Paterson G S 1978 *J. Fluid Mech.* 85 305